Analytical Formulas for In-Situ Combustion

A.A. Mailybaev, Institute of Mechanics, Moscow State Lomonosov University;
J. Bruining, SPE, Delft University of Technology;
and **D. Marchesin,** Instituto Nacional de Matemática Pura e Aplicada, Rio de Janeiro

Summary

There is a renewed interest in using combustion to recover medium- or high-viscosity oil. Despite numerous experimental, numerical, and analytical studies, the mechanisms for incomplete fuel combustion or oxygen consumption are not fully understood. Incomplete oxygen consumption may lead to low-temperature oxidation reactions downstream. This paper shows that these features emerge in a relatively simple 1D model, where air is injected in a porous medium filled with inert gas, water, and an oil mixture consisting of precoke, medium oil, and light oil. Precoke is a component that is dissolved in the oil but has essentially the same composition as coke. At high temperatures, precoke is converted to coke, which participates in high-temperature oxidation. At high temperatures, medium-oil components are cracked, releasing gaseous oil. Light-oil components and water are vaporized. The model possesses an analytical solution, which was obtained by a concept introduced by Zeldovich et al. (1985). This concept, which underlies most analytical approaches such as the reaction-sheet approximation and large-activation-energy asymptotics, entails that reaction can occur only in a very small temperature range because of the highly nonlinear nature of the Arrhenius factor. For a temperature below this range, the reaction rate is too slow, and for temperatures above this range, the reaction rate is so fast that either the fuel or oxygen concentrations become zero. The model results, in the absence of external heat losses, show that there are two combustion regimes in which coke or oxygen is partially consumed. In one regime, the reaction zone moves in front of the heat wave; whereas, in the other regime, the order of the waves is reversed. There are also two combustion regimes in which the coke and oxygen are completely consumed. Also, here the reaction zone can move in front of or at the back of the heat wave. Each combustion regime is described by a sequence of waves; we derive formulas for parameters in these waves. We analyze our formulas for typical in-situ-combustion data and compare the results with numerical simulation. The main conclusion is that mainly two key parameters (i.e., the injected oxygen mole fraction and the fuel concentration) determine the combustion-front structure and when either incomplete oxygen consumption or incomplete fuel consumption occurs in the high-temperature oxidation zone.

Introduction

One of the options to recover medium- or high-viscosity oil (i.e., oil with a viscosity higher than 10^2 cp) is the application of air injection (Castanier and Brigham 1997; Castanier and Brigham 2003; Kuhn and Koch 1953), leading to oil combustion. The most critical issue for oil combustion is incomplete consumption of oxygen; from a perspective of safety, it can lead to possible hazardous conditions at the production well (Bowes and Thomas 1966). Another issue is extinction, which is related to incomplete fuel or oxygen consumption. Finally, there are efficiency considerations also tied up with incomplete consumption. Until now, no analytical solutions have been published for 1D in-situ-combustion processes that involve detailed wave structure including cracking, solid-fuel consumption, and vaporization. Even in one dimension, this is not a trivial problem because processes such as combustion and cracking occur in narrow regions, yielding a difficult multiscale problem (Gerritsen and Durlofsky 2005; Kristensen et al. 2007).

For various combustion conditions, analytical studies of combustion waves in porous media containing solid fuel were performed by Aldushin et al. (1996, 1997, 2006) and Wahle et al. (2003). These studies used the sheet approximation, assuming that the reaction region is very thin. Therein, the reaction-leading and reaction-trailing structures of the combustion wave were studied in conjunction with the possibility of partial or complete consumption of reactants. A similar asymptotic approach based on small parameter expansion was developed by Schult et al. (1996) and later used for in-situ-combustion problems by Akkutlu and Yortsos (2000). Periodic and other nonsteady combustion regimes were investigated by Bayliss and Matkowsky (1994), Matkowsky and Sivashinsky (1978), and Schult et al. (1998). The influence of solid conversion (Byrne and Norbury 1997), heat losses (Akkutlu and Yortsos 2003), heterogeneity of porous medium (Akkutlu and Yortsos 2005), multiple reactions (Akkutlu and Yortsos 2004; Adagulu and Akkutlu, 2007), and vaporization (Bruining et al. 2009) was analyzed. A wave-structure analysis within a thin combustion zone is necessary. This represents the main mathematical difficulty of such studies. When water is injected together with air, the combustion wave can be driven by the cooling rate caused by the cold-water injection (Dietz and Weijdema 1968; Weijdema 1968) rather than by the fuel-consumption rate.

A number of pioneering papers have built up our present understanding of the oil-combustion process. Application of air injection is one of the oldest enhanced-oil-recovery (EOR) techniques, but soon afterward it became less important than steam injection and steam soak. However, oil combustion as a recovery technique has provoked a steady stream of papers in the petroleum-engineering literature. The essence of the process was already established by Ramey (1954). He proposed that the oxygen in the air burns the heavier components of oil (Abou Kassem et al. 1986; Akin et al. 2000; Kok and Karacan 2000; Lin et al. 1987; Lin et al. 1984), generating a heat wave leading to vaporization of lighter components that are produced.

High-temperature oxidation (HTO) and low-temperature oxidation (LTO) are the dominant phenomena for modeling of combustion. Our study focuses on HTO and includes cracking and vaporization of heavy components, as has been described by Abu-Khamsin et al. (1988). This paper focuses on one step in improving understanding of the whole combustion phenomenon (i.e., if HTO occurs with complete oxygen consumption, no LTO will occur). Cracking and vaporization are an essential part of the HTO-reaction process and contribute to its efficiency.

Mamora and Brigham (1995) conclude that either pure HTO occurs in which all oxygen is consumed or that combustion in the HTO zone is incomplete and thus inefficient, leading to LTO, which generates oxygenated hydrocarbons with high viscosities. Thus, it is important to study how much oxygen is consumed in the HTO process. The conditions for which this occurs are studied in depth in this paper. Mamora (1995) states that, if incomplete oxygen consumption occurs at the HTO reaction zone, LTO will occur downstream, leading to an inefficient HTO combustion process. He et al. (2005) study the catalytic effects of naturally occurring minerals. These may stimulate HTO more than LTO and, thus, may improve the overall efficiency of the process. Akkutlu and Yortsos (2004) analyze the situation of coupled LTO/HTO

This paper (SPE 129904) was accepted for presentation at the SPE Symposium on Improved Oil Recovery, Tulsa, 24–28 April 2010, and revised for publication. Original manuscript received for review 9 February 2010. Revised manuscript received for review 26 August 2010. Paper peer approved 31 August 2010.

reactions and identify the parameter space for which heat losses are minimized in this way.

In the 1D framework, oil downstream of the HTO is cracked and vaporized and moves toward the production well. Thus, although vaporization and cracking are not dominant processes that drive the combustion, their analysis in the fine structure of the combustion wave is important in oil-recovery applications. The goal of our work is to identify various combustion regimes in a model that includes solid-fuel consumption, cracking, and evaporation (i.e., the regimes for which the reaction front is downstream or upstream of the heat wave and the fuel or oxygen consumption is complete or incomplete).

We analyze the model that includes a three-pseudocomponent crude oil for in-situ combustion. The pseudocomponents are distinguished according to the types of reaction in which they participate—oxidation, cracking, or vaporization. We approximate the combustion region in the whole solution as a sequence of waves traveling with constant speeds, separated by regions where the properties are almost homogeneous. For the time being, we take the reservoir state ahead of the combustion/cracking/evaporation wave as known. Otherwise, one needs an extension of the present model to flow, condensation, and slow-oxidation reactions in the reservoir at relatively low temperatures, which can be solved as a separate problem. We use a concept introduced by Zeldovich (Zeldovich et al. 1985) for the analysis of combustion waves, which implies that combustion occurs in a very small temperature window. For temperatures that are too low, the Arrhenius factor shows that the reaction rates become too slow. For temperatures that are too high, the reaction rate becomes so fast that the combustion mixture will become depleted of an essential reactant. We derive explicit formulas for dependent variables in the combustion wave and classify possible combustion regimes. In particular, explicit conditions for complete or incomplete oxygen consumption in the HTO process are given. Note that similar conditions were studied by Schult et al. (1996).

Stability and accuracy of the analytical solution were checked by simulations for representative problem parameters. Though the Zeldovich concept was widely used before for in-situ-combustion problems, we succeeded in simplifying both the derivation and the final form of the result, keeping the same order of accuracy. The key conclusion of the paper is that mainly two parameters (i.e., the injected oxygen mole fraction and the fuel concentration) determine the combustion-front structure and when either incomplete oxygen consumption or incomplete fuel consumption occurs in the HTO zone. Here, we do not study the LTO that may occur in the case of incomplete oxygen consumption.

The structure of the paper is as follows. First, we describe the model. Next, we discuss combustion regimes, providing explicit conditions for each regime and parameters of combustion waves. Subsequently, we give the results of numerical calculations with typical reservoir data for in-situ combustion. We end with some conclusions. Appendices A through D provide some sketches of the calculations; a more-detailed treatment can be found in Mailybaev et al. (2010).

Model

We study forward combustion when a gaseous oxidizer (air) is injected into a porous medium (e.g., a rock cylinder thermally insulated against lateral heat losses and filled with gas, some crude oil, and water). We consider medium-viscosity oil. The mobility of any components other than gas will be ignored because it is assumed that the speed of the reaction wave substantially exceeds the speed of any liquids. We express the concentrations and reaction rates in mass per unit pore volume and mass per unit pore volume per unit time, respectively.

The oil in the reservoir contains various components—saturates, aromatics, resins, and asphaltenes. The heaviest components (e.g., asphaltenes) are converted into coke in the high-temperature zone [see, however, Akin et al. (2000) for more details]. We use the word precoke to denote these components. We disregard both the formation of gaseous components during this conversion process and the heat of reaction associated with the splitting (Abu-Khamsin et al. 1988). Therefore, we will consider the precoke as well as its product (coke) as a single pseudocomponent with carbon concentration n_h in kg/m^3. The combustion of coke in the presence of oxygen gives rise to the highest temperatures present in the combustion process. It is called HTO. We model HTO combustion as a single reaction

$$C + O_2 \rightarrow CO_2. \qquad (1)$$

The other components—saturates, aromatics and resins—are lumped into two pseudocomponents (i.e., light and medium oil). The light components are vaporized ahead of the combustion zone. The concentration of the light oil is denoted by n_v in kg/m^3. The average molar weight of the light-oil pseudocomponent is denoted by M_v in kg/mol. If water is present, we lump it into the light-oil component because they vaporize in the same region. The concentration of the medium-oil pseudocomponent is denoted by n_c in kg/m^3. As temperature increases, the medium oil cracks into various components, which are released as vapor (i.e., they do not form coke). The average molar weight of these vapor components is denoted by M_c in kg/mol.

The three pseudocomponents (precoke/coke, medium oil, and light oil) are distinguished according to the corresponding process: HTO, cracking, and vaporization, respectively. Transport of oil by convection is disregarded, as explained previously. Therefore, it is possible to write the rate of change of oil concentrations in terms of the reaction rates W in (kg/m^3)/s, as

$$\frac{\partial n_h}{\partial t} = -W_h,$$

$$\frac{\partial n_c}{\partial t} = -W_c,$$

$$\frac{\partial n_v}{\partial t} = -W_v. \qquad (2)$$

The gas phase contains oxygen, gaseous oil, steam, combustion products (carbon dioxide), and initial inert gas. In some combustion regimes, oxygen may be present in the gas together with gaseous light oil, leading to an oxidation reaction. However, as we will see, gaseous light oil appearing because of cracking or vaporization is immediately transported to colder zones, where the oxidation rate is so small that it can be ignored. This is why we do not need to distinguish the different components of gaseous oil. In the gas composition, we will distinguish the mole fraction Y of oxygen and the remaining gas fraction $1-Y$ that consists of vaporized oil, steam, combustion products, and the initial inert gas. The mass-balance equations for the gas fractions, ignoring diffusion, are

$$\frac{\partial \phi (1-Y)\rho}{\partial t} + \frac{\partial (\rho u - \rho u Y)}{\partial x} = \frac{W_h}{M_h} + \frac{W_c}{M_c} + \frac{W_v}{M_v} \qquad (3)$$

and

$$\frac{\partial \phi Y \rho}{\partial t} + \frac{\partial \rho u Y}{\partial x} = -\frac{W_h}{M_h}, \qquad (4)$$

where ϕ is porosity, ρu is molar gas flux, $\rho u Y$ is molar oxygen flux, $\rho = P_{tot}/RT$ in mol/m^3 is the molar density of gas at the prevailing pressure P_{tot} in Pa, u in m/s is the gaseous-phase Darcy velocity, $M_h = 0.012$ kg/mol is the carbon molar mass. In Appendix D, we will show that correction because of gas diffusion may be small, even if the diffusion is large. Pressure variations are assumed to be small, so we take P_{tot} = constant. The sum of Eqs. 3 and 4 gives the mass balance for the total gas:

$$\frac{\partial \phi \rho}{\partial t} + \frac{\partial \rho u}{\partial x} = \frac{W_c}{M_c} + \frac{W_v}{M_v}. \qquad (5)$$

The W_h term cancels out because the coke oxidation reaction (Eq. 1) produces no net gas.

Heat losses in the field are small, and, therefore, experiments have been conducted (Gutierrez et al. 2009) that compensate for them. Neglecting heat losses, we write the heat equation as

$$\frac{\partial C_m T}{\partial t}+\frac{\partial c_g\left(T-T_{st}\right)\rho u}{\partial x}=\lambda\frac{\partial^2 T}{\partial x^2}+Q_h W_h-Q_c W_c-Q_v W_v. \quad \ldots(6)$$

Here, T in K is the temperature and T_{st} = 293.15 K is our reference temperature; λ in W/mK is the thermal conductivity of the porous medium; and C_m in J/m^{3}K is the heat capacity per unit volume of the porous medium, which, for simplicity, is taken to be approximately equal to the constant heat capacity of the rock. We disregard gas, water, and oil heat capacities compared to rock heat capacity in the accumulation term because, in all cases of interest, the amount of liquids is small, leading to a small error (~10%). The gas heat capacity c_g in J/mol·K is taken as $c_g \approx 3.5R$, ignoring small variations of the heat capacity among different gas components. The heats Q_h, Q_c, and Q_v in J/kg correspond to HTO reaction, cracking, and vaporization of light oil/water, respectively. They are all positive, except in the rare cases when Q_c is negative.

Arrhenius' law and the assumption of a linear dependence on the fuel concentration and oxygen concentration lead to

$$W_h = K_h Y n_h \exp\left[-E_h/(RT)\right], \quad \ldots(7)$$

with activation energy E_h in J/mol and frequency factor K_h in 1/s (Abu-Khamsin et al. 1988). Here, we follow Bousaid and Ramey (1968), where a linear dependence for oxygen and fuel was assumed. We will not need an expression for the vaporization rate because it affects only the internal structure of the condensation wave, which is not relevant here. For the cracking-reaction rate, it is suggested by the same authors to use

$$W_c = K_c n_c \exp\left[-E_c/(RT)\right], \quad \ldots(8)$$

with activation energy E_c and frequency factor K_c (Bousaid and Ramey 1968). Note that the temperature dependence is dominant in Eqs. 7 and 8, and our method can be modified easily for different kinetic exponent dependencies of the reactants.

The variables to be found are the temperature T; the concentrations n_h, n_c, n_v, and Y; and the Darcy velocity u. All the coefficients in the equations (e.g., C_m, c_g, λ) are assumed to be constant. The molar flux of injected air is $(\rho u)_{\text{inj}}$. The injected oxygen flux is $(\rho u Y)_{\text{inj}}$, with an oxygen mole fraction Y_{inj}. Ignition occurs at the entrance of the reservoir, and combustion propagates in the same direction as the injected air.

Combustion Regimes

In this section, we provide a quantitative analytical description for possible in-situ-combustion regimes that have the form of sequences of waves traveling with constant speeds. Derivations of these formulas are given in Appendices A through C.

In-situ combustion generates a wide hot region where the heat released in the HTO reaction is stored. However, the region where the HTO reaction takes place is very thin. It is conventional to distinguish between a reaction-leading combustion structure, where the HTO region is ahead of the hot zone, and a reaction-trailing structure, where the HTO region is behind of the hot zone (Wahle et al. 2003).

Reaction-Leading Structure. The reaction-leading structure is shown in **Fig. 1.** It contains a reaction wave traveling with speed ν followed by a slower thermal wave, with speed [see, e.g., Bruining et al. (2009)]

$$\upsilon_T = c_g\left(\rho u\right)_{\text{inj}} / C_m. \quad \ldots(9)$$

because cold gas is injected. The hot zone between these waves contains only injected gas. The reaction wave contains several thin regions, shown in **Fig. 2.** There is a thin HTO region at the left, where coke oxidation occurs, with wider regions further to the right where cracking and vaporization occur. The presence of a hot zone containing oxygen behind the reaction wave ensures that all coke is consumed in the HTO reaction. Oxygen consumption is not necessarily complete, so the HTO reaction is coke-controlled. In the presence of oxygen passing through the combustion zone, slow oxidation may occur farther downstream, which we disregard in the current study. Ahead of the reaction wave, the temperature drops to the vapor-zone temperature T_v. The vapor zone contains oil and water in both liquid and gaseous forms. When the gas reaches the original cold reservoir, part of the oil vapor and water condenses. This solution structure is called reaction-leading because combustion occurs ahead of the hot zone.

In this paper, we are interested only in the part of the whole structure upstream of the vapor zone. In the vapor zone, the concentrations n_h^*, n_c^*, and n_v^*, and the temperature T_v are determined by the condensation and flow processes far downstream (right) of the reaction wave, which represent a separate problem. In our study of combustion, we assume these quantities to be known. The unknown parameters of the reaction wave to be determined are the temperature T_h, the reaction wave speed ν, the gas-flux change in the wave, and the amount of oxygen that passes through unburned.

The oil vapor and steam released in the reaction wave because of cracking and vaporization increase the molar gas flux by $\nu n_c^* / M_c$ and $\nu n_v^* / M_v$, respectively. In the vapor zone, the gas flux is given by

$$\left(\rho u\right)_v = \left(\rho u\right)_{\text{inj}} + \upsilon\left(n_c^* / M_c + n_v^* / M_v\right). \quad \ldots(10)$$

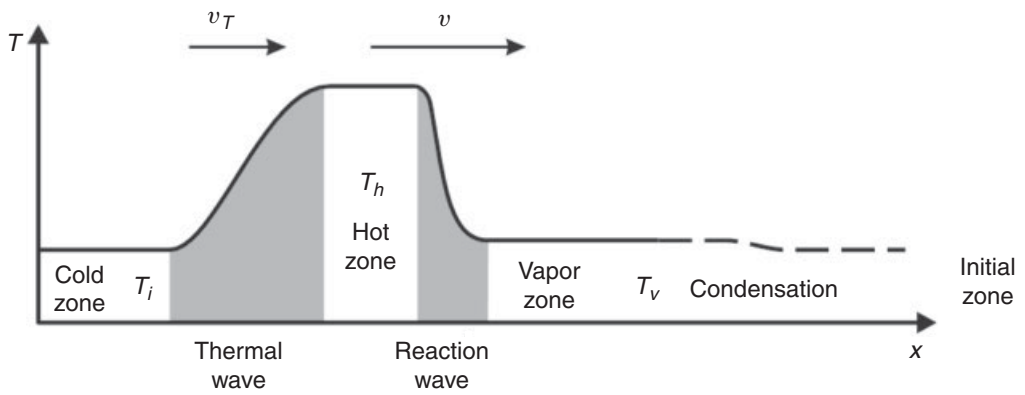

Fig. 1—Reaction-leading structure. The reaction wave is faster than the thermal wave. The cold and hot zones contain air. The vapor zone contains oil, water, and gas with oil vapor, steam, and combustion products.

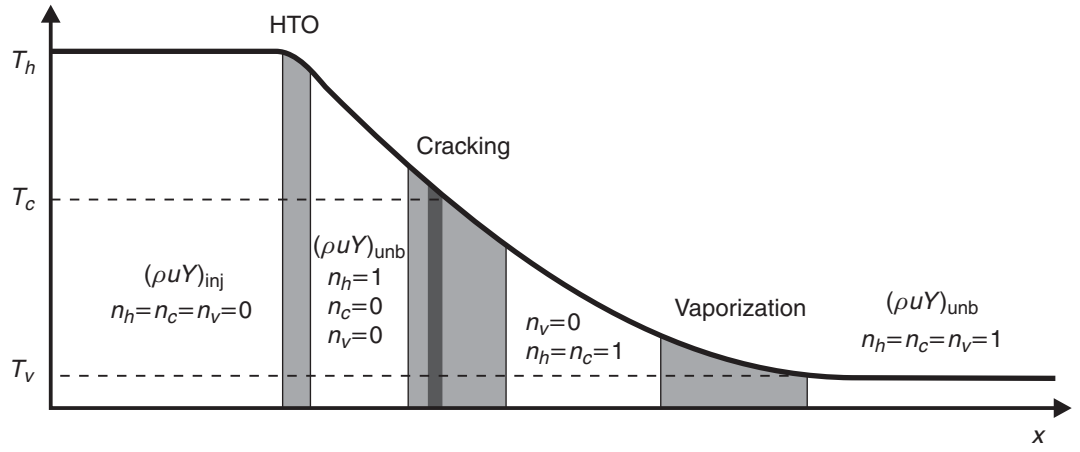

Fig. 2—Reaction-wave internal structure for reaction-leading case: HTO, cracking, and vaporization regions. Cracking of each component occurs in a thin region within the cracking zone. The values of oxygen flux ρuY and oil-component concentrations n_h, n_c, and n_v are specified in different regions.

Analysis of the combustion zone is carried out using the Zeldovich approach, as described in Appendix A. These results are used in Appendix B to determine the reaction-wave parameters with relative accuracy of order Z_h^{-1}, the inverse Zeldovich number defined in Eq. A-2. We present the final results in the case when the contributions of cracking and vaporization in the total heat balance are small compared to the HTO reaction.

There are two different combustion regimes with reaction-leading structure. They correspond to complete consumption of coke and either complete or partial consumption of oxygen in the HTO reaction. In the regime of complete oxygen consumption, the wave speed and highest temperature in the wave are based on mass- and heat-balance considerations:

$$\upsilon = \frac{(\rho uY)_{\text{inj}} M_h}{n_h^*}$$

$$T_h = T_v + \frac{\upsilon Q_h n_h^*}{\upsilon C_m - c_g (\rho u)_{\text{inj}}}. \quad \ldots\ldots\ldots\ldots\ldots\ldots\ldots\ldots (11)$$

The first expression in Eq. 11 states that υ is the fuel-consumption rate, and the second equation expresses that the combustion heat is used to heat up the space between the thermal wave traveling at a speed v_T and the combustion front traveling at speed υ. Complete oxygen consumption occurs only if the reaction zone is sufficiently long and the temperature and reaction rate are sufficiently high; i.e.,

$$\frac{\lambda R T_h^2 K_h n_h^*}{E_h Q_h Y_{\text{inj}} (\rho u)_{\text{inj}}^2 M_h^2} \exp\left(-\frac{E_h}{RT_h}\right) > 1. \quad \ldots\ldots\ldots\ldots\ldots\ldots\ldots\ldots (12)$$

If the condition of Eq. 12 is not satisfied, a considerable part of the oxygen is not consumed in the reaction. This is the situation we address now. We can use the second expression at Eq. 11 also for incomplete oxygen consumption, written as

$$\upsilon = \frac{c_g (\rho u)_{\text{inj}}}{C_m - Q_h n_h^* / (T_h - T_v)}. \quad \ldots\ldots\ldots\ldots\ldots\ldots\ldots\ldots (13)$$

The highest temperature T_h in the wave in the case of incomplete oxygen consumption is determined implicitly by

$$\frac{\lambda R T_h^2 K_h Y_{\text{inj}}}{E_h Q_h n_h^* \upsilon^2} \exp\left(-\frac{E_h}{RT_h}\right) = 1, \quad \ldots\ldots\ldots\ldots\ldots\ldots\ldots\ldots (14)$$

where υ must be substituted from Eq. 13. This implicit equation can be solved by using a numerical program for a single nonlinear equation. The lower bound for T_h to be used in the program is

$$T_h > T_v + \frac{Q_h n_h^*}{C_m - c_g n_h^* / (Y_{\text{inj}} M_h)}. \quad \ldots\ldots\ldots\ldots\ldots\ldots\ldots\ldots (15)$$

Equating the consumption of oxygen to the consumption of coke, we obtain

$$(\rho uY)_{\text{inj}} - (\rho uY)_{\text{unb}} = \upsilon n_h^* / M_h. \quad \ldots\ldots\ldots\ldots\ldots\ldots\ldots\ldots (16)$$

In this way, we can calculate the mole fraction of unburned oxygen Y_{unb}. Requiring that Y_{unb} in Eq. 16 be nonnegative together with the condition $v_T < \upsilon$ and v_T from Eq. 9, we can show that

$$(\rho uY)_{\text{inj}} > v_T \frac{n_h^*}{M_h} = \frac{(\rho u)_{\text{inj}} c_g}{C_m} \frac{n_h^*}{M_h}$$

or

$$Y_{\text{inj}} > \frac{c_g n_h^*}{C_m M_h}. \quad \ldots\ldots\ldots\ldots\ldots\ldots\ldots\ldots\ldots\ldots (17)$$

This condition is satisfied in most practical situations unless the injected gas contains very little oxygen.

Applying the concept of Zeldovich in the cracking zone shows that the temperature T_c satisfies the equation

$$\frac{R T_c^2 K_c}{2\upsilon E_c |T_c'|} \exp\left(-\frac{E_c}{RT_c}\right) = 1, \quad \ldots\ldots\ldots\ldots\ldots\ldots\ldots\ldots (18)$$

where

$$T_c' = -Q_h n_h^* \upsilon / \lambda + C_m (\upsilon - v_T)(T_h - T_c) / \lambda. \quad \ldots\ldots\ldots\ldots\ldots\ldots (19)$$

Using Eq. 19, Eq. 18 can be solved numerically, furnishing the cracking temperature T_c. This is an average cracking temperature, when K_c and E_c are effective cracking kinetic coefficients. In a more realistic model, each medium-oil component cracks in a thin region near the corresponding temperature T_c; see Fig. 2 (thin dark interval within a wider cracking zone). This temperature is determined by the same equations (Eqs. 18 and 19), where K_c and E_c are the kinetic coefficients corresponding to this specific component. The position of the cracking region in the wave can also be computed for each component, as shown in Appendix B.

Of course, for our solution to be correct, it is important that $T_c < T_h$ for each medium-oil component. Otherwise, medium oil remains in the HTO zone and participates in the HTO reaction.

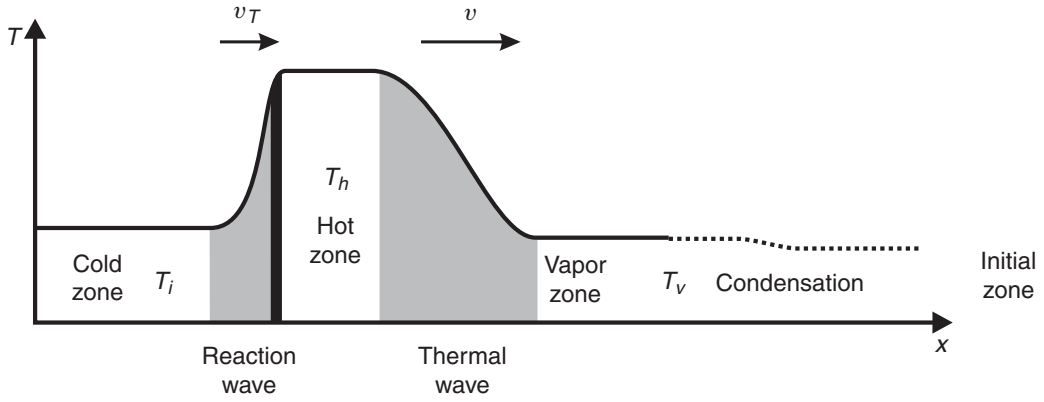

Fig. 3—Reaction-trailing structure. The reaction wave is slower than the thermal wave. A thin region where the HTO reaction occurs is shown in black. The cold zone contains air. The hot zone contains coke and gas with combustion products. The vapor zone contains oil, steam, and gas with oil vapor, steam, and combustion products.

Reaction-Trailing Structure. The reaction-trailing structure is shown in **Fig. 3.** The coke-oxidation reaction occurs in a slow reaction wave traveling with speed v. The temperature in this wave changes from a high-value T_h in the hot zone downstream to the injected air temperature T_i upstream. The cracking reaction and oil vaporization take place in another wave traveling with higher speed $v_T > v$. If there were neither medium oil nor light oil/water in the reservoir, this wave would be just a thermal wave with speed determined by Eq. 9. The hot region between the two waves contains coke with concentration n_h^* but neither medium oil nor light oil/water. As in the preceding subsection, we assume that the oil-component concentrations n_h^*, n_c^*, and n_v^* and the temperature T_v in the vapor zone upstream of the thermal-wave region are given.

Because the hot region upstream of the reaction wave contains coke, oxygen is consumed completely in the HTO reaction. Coke consumption is not necessarily complete, so the HTO reaction is oxygen controlled. This solution structure is called reaction trailing because combustion occurs downstream of the hot zone. The existence of the hot zone between the reaction and thermal wave ensures that complete cracking of the medium oil occurs upstream of the reaction wave.

The only reaction in the reaction wave is coke oxidation. There are two different combustion regimes in the reaction-trailing structure, corresponding to either complete or partial consumption of coke in the HTO reaction. The derivation is similar to that for the reaction-leading structure, and we do not go into details (available in Appendix C). In the regime of complete coke consumption, the wave speed and the highest temperature in the reaction wave are

$$v = \frac{(\rho u Y)_{\text{inj}} M_h}{n_h^*}$$

$$T_h = T_i + \frac{v Q_h n_h^*}{c_g (\rho u)_{\text{inj}} - v C_m}. \quad \ldots\ldots\ldots\ldots\ldots\ldots\ldots\ldots (20)$$

This regime is determined by the condition of Eq. 12.

If Eq. 12 is not satisfied, the unburned concentration of coke is given by n_h^{unb}. In this case, the wave speed is related to the combustion temperature T_h by

$$v = v_T - \frac{Q_h (\rho u Y)_{\text{inj}} M_h}{C_m (T_h - T_i)}. \quad \ldots\ldots\ldots\ldots\ldots\ldots\ldots\ldots (21)$$

The temperature T_h is determined implicitly by

$$\frac{\lambda R T_h^2 K_h n_h^*}{E_h Q_h (\rho u)_{\text{inj}}^2 Y_{\text{inj}} M_h^2} \exp\left(-\frac{E_h}{R T_h}\right) = 1. \quad \ldots\ldots\ldots\ldots\ldots\ldots\ldots\ldots (22)$$

This equation is solved using a numerical solver for a single algebraic equation, with lower bound

$$T_h > T_i + \frac{Q_h n_h^*}{c_g n_h^* / (Y_{\text{inj}} M_h) - C_m}. \quad \ldots\ldots\ldots\ldots\ldots\ldots\ldots\ldots (23)$$

The unburned-coke concentration left behind the reaction wave is

$$n_h^{\text{unb}} = n_h^* - (\rho u Y)_{\text{inj}} M_h / v. \quad \ldots\ldots\ldots\ldots\ldots\ldots\ldots\ldots (24)$$

The thermal-wave speed is approximately equal to the value in Eq. 9. However, cracking and vaporization that occur in this wave slightly decrease the value in Eq. 9. The gas flux in the vapor zone is given similarly to that in Eq. 10 as

$$(\rho u)_v = (\rho u)_{\text{inj}} + v_T (n_c^* / M_c + n_v^* / M_v). \quad \ldots\ldots\ldots\ldots\ldots\ldots\ldots\ldots (25)$$

Requiring that Eq. 24 be nonnegative and using the condition $v_T > v$ with v_T from Eq. 9, we obtain

$$Y_{\text{inj}} < c_g n_h^* / (C_m M_h). \quad \ldots\ldots\ldots\ldots\ldots\ldots\ldots\ldots\ldots\ldots (26)$$

This is opposite to Eq. 17. It is satisfied when the coke concentration is large or the oxygen concentration in the injected air is small.

We conclude that the reaction-leading combustion wave occurs under the condition of Eq. 17. Otherwise, we have the reaction-trailing structure. The regime with complete consumption of coke and oxygen in the HTO is determined by Eq. 12, where T_h is given by Eq. 11 for the reaction-leading structure and by Eq. 20 for the reaction-trailing structure. If Eq. 12 is not satisfied, a considerable part of the oxygen or the coke is not consumed, respectively, in the reaction-leading and reaction-trailing cases.

In-Situ Combustion for Typical Reservoir Parameters

Consider the typical reservoir data in **Table 1.** The numbers quoted correspond to octene (C_8H_{16}) as an effective light-oil component, hexadecene ($C_{16}H_{32}$) as a medium-oil component, and average vaporization heat Q_v for a liquid mixture with equal light-oil and water concentrations in the vapor zone.

Assume that air with oxygen fraction $Y_{\text{inj}} = 0.21$ is injected into the reservoir. Eq. 17 is satisfied for precoke concentrations $n_h^* < 173$ kg/m^3 in the vapor zone. This is the case of the reaction-leading wave structure. **Fig. 4** shows the reaction-wave parameters vs. the initial precoke concentration n_h^* in kg/m^3 when the other parameters in the vapor zone are taken as $n_c^* = 100$ kg/m^3, $n_v^* = 60$ kg/m^3, and $T_v = 77$°C. Complete coke and oxygen consumption in the HTO reaction occurs for high precoke concentrations $n_h^* > 35.5$ kg/m^3,

TABLE 1—NOMENCLATURE, UNITS, AND TYPICAL VALUES OF DIMENSIONAL PARAMETERS FOR IN-SITU COMBUSTION

Parameter	Meaning	Value
Q_h	HTO reaction enthalpy	3.28×10^4 kJ/kg
Q_c	Cracking reaction enthalpy	339 kJ/kg
Q_v	Vaporization heat	1280 kJ/kg
E_h	Activation energy (HTO)	180 kJ/mol (Smith 1978)
K_h	Pre-exponential factor (HTO)	3.05×10^6 1/s (Smith 1978)
E_c	Activation energy (cracking)	250 kJ/mol (Pant and Kunzru 1996)
K_c	Pre-exponential factor (cracking)	6×10^{13} 1/s (Pant and Kunzru 1996)
R	Gas constant	8.314 J/mol K
C_m	Heat capacity of rock	2×10^3 kJ/m^3 K
λ	Thermal conductivity of rock	0.87 W/mK
c_g	Heat capacity of gas	3.5R J/mol K
P_{tot}	Prevailing pressure of gas	10^5 Pa (1 atm)
u_{inj}	Darcy velocity of injected gas	1.16×10^{-3} m/s (100 m/d)
M_h	Molar weight of carbon	0.012 kg/mol
M_c	Average molar weight of cracked oil	0.112 kg/mol
M_v	Average molar weight of liquid oil and water	0.065 kg/mol
$T_i = T_{st}$	Injected-gas temperature	293.15 K

as found by checking the inequality of Eq. 12. For lower precoke concentrations, a considerable part of the injected oxygen passes through the reaction zone, as shown in Fig. 4. The transition from complete- to partial-oxygen-consumption regime is characterized by an abrupt change in the dependence of the variables relative to the coke concentration n_h^*. The curves in Fig. 4 were computed using Eq. 11 for complete consumption of oxygen and Eqs. 13, 14, and 16 for partial consumption of oxygen.

Fig. 4b shows the velocities of the combustion wave v and thermal wave v_T together with the curve for Y_{inj}. For low values of n_h^*, we observe that there is a point where the speeds coincide, $v_T = v$; however, in this case, $Y_{unb} = Y_{inj}$, meaning there is essentially no combustion. Also, for the large value $n_h^* = 173$ kg/m^3 (outside Fig. 4b), there is another point with coinciding speeds. It is the resonance point, with complete oxygen consumption $Y_{unb} = 0$ lying on the resonance line in **Fig. 5.**

Calculations using Eqs. B-1 and B-4 in Appendix B instead of Eq. 13 verify that changes in medium-oil and light-oil/water concentrations have minor influence on the combustion and cracking temperatures T_h and T_c, respectively. The speed v of the reaction wave decreases slightly with an increase of medium-oil and light-oil/water concentrations.

Consider now the same reservoir parameters in the vapor zone but an injected gas with very low initial oxygen fraction $Y_{inj} = 0.025$. The numerical results are shown in **Fig. 6.** The condition of Eq. 17 is satisfied for precoke concentrations $n_h^* < 20.6$ kg/m^3 and corresponds to the reaction-leading structure discussed in the corresponding section. Higher concentrations lead to the reaction-trailing wave structure, and calculations use the formulas of the corresponding section. These two cases are separated by a resonance point, where the speeds of the two waves coincide: $v = v_T$. The complete coke/oxygen-consumption regime is determined by the inequality Eq. 12 and corresponds to $14.5 < n_h^* < 44.9$ kg/m^3. Temperatures in this region become very high. On the contrary, the partial-oxygen ($n_h^* < 14.5$ kg/m^3) and partial-coke ($n_h^* > 44.9$ kg/m^3) -consumption regimes are characterized by almost constant combustion temperature. The dependence of the reaction wave parameters on n_h^* possesses a singularity when the regime changes. Numerical results were obtained by using Eqs. 11 or 20 for complete-oxygen and -coke consumption; Eqs. 13, 14, and 16

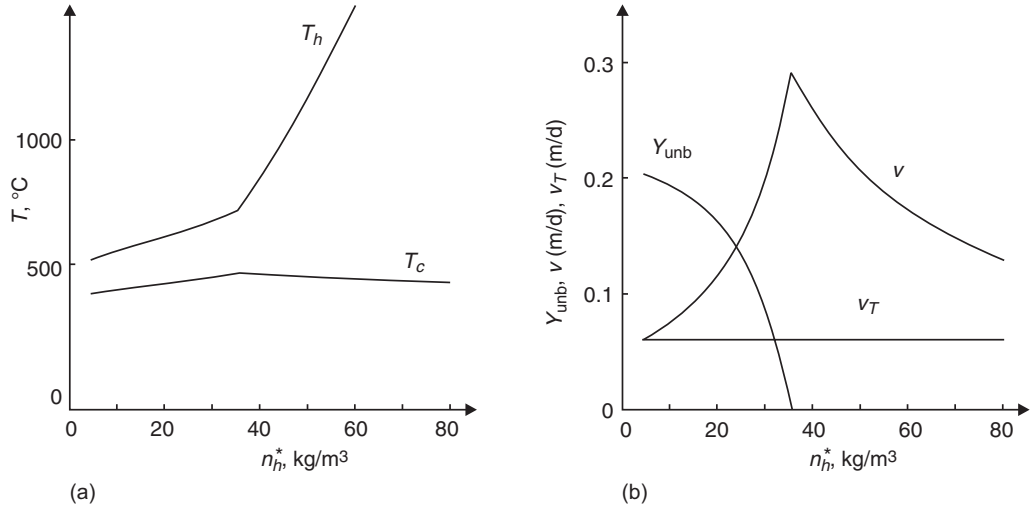

Fig. 4—Reaction-wave parameters depending on precoke concentration n_h^* in kg/m^3, with $n_c^* = 100$ kg/m^3 and $n_v^* = 60$ kg/m^3 for injection of air with 21% oxygen. The vapor-zone temperature is $T_v = 77$°C. The hot-zone temperature is T_h in °C. The cracking temperature is T_c in °C. The HTO and thermal-wave speeds are denoted, respectively, by v and v_T in m/d. The unburned oxygen fraction is Y_{unb}.

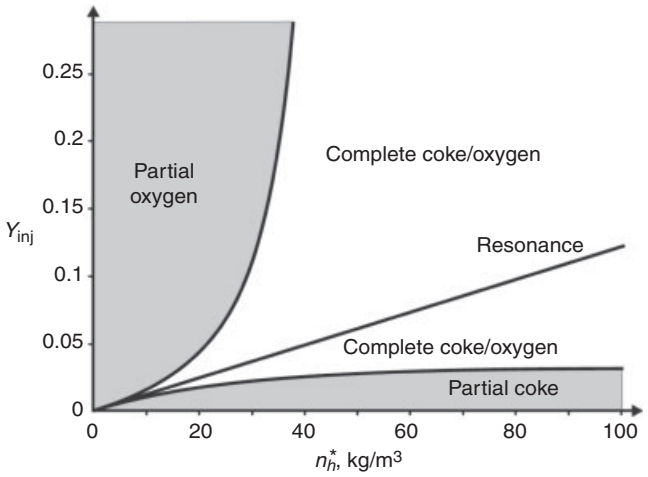

Fig. 5—Chart of combustion regimes for different coke concentrations n_h^* in kg/m³ and injected-oxygen fractions Y_{inj}. Resonant states form a straight line that separates combustion regimes with different wave structures: reaction-leading (above the line) and reaction-trailing (below the line). The gray regions correspond to combustion regimes with partial oxygen and partial coke consumption. The white region corresponds to the complete coke and oxygen consumption.

for partial oxygen consumption; and Eqs. 21, 22, and 24 for partial coke consumption.

Fig. 5 presents a chart with different combustion regimes in the (n_h^*, Y_{inj}) plane: coke concentration vs. oxygen fraction in the injected air. The boundary between the reaction-leading (Eq. 17) and reaction-trailing (Eq. 26) combustion structures is determined by the straight resonance line $Y_{inj} = n_h^* c_g / (C_m M_h)$. The boundary of the regime with complete consumption of coke and oxygen, shown white in Fig. 5, is determined by Eq. 12 written as an equality. Here, we must substitute T_h from Eq. 11 to determine the boundary with the domain corresponding to partial oxygen consumption, or T_h from Eq. 20 to determine the boundary with the domain corresponding to partial coke consumption. There is also a boundary corresponding to extinction at small coke concentration n_h^*. This branch of points is characterized by low oxygen consumption [see Mailybaev et al. (2010) for details] and is not included in Fig. 5. Such extinction occurs in situations where the combustion heat $Q_h n_h^*$ is close to the heat $Q_c n_c^* + Q_v n_v^*$ necessary for cracking and vaporization and the speeds of the two waves coincide, $v_T = v$; see Eqs. B-1 and B-4. The speed v gets close to v_T also for very small injected-oxygen fractions Y_{inj}, as one can show by using Eqs. 21 and 22. The chart of combustion regimes has the qualitative form shown in Fig. 5 for a wide range of parameters. Recall that the coke concentration n_h^* depends on the processes downstream of the reaction wave. The determining mechanism here is the condensation of light oil and steam from the gas in the cold zone downstream. In turn, the condensed gas affects the quantity and properties of the oil left to participate in the combustion. Unless the oxygen concentration in the injected gas is very low, the reaction-leading structure occurs, and oxygen breakthrough in the HTO region is possible if n_h^* is not large enough, as shown in Fig. 5.

Computations show that a change of the injected-gas speed u_{inj} has minor influence on the reaction-wave structure. The reaction-wave speed v is approximately proportional to μ_{inj}. The HTO temperature in the complete coke and oxygen consumption regime does not depend on the gas speed. Only increases of several orders magnitude in u_{inj} have noticeable influence on HTO and cracking temperatures in the cases of partial-oxygen- or partial-coke-consumption regimes; the region of complete coke/oxygen consumption on the plane (n_h^*, Y_{inj}) widens.

We performed direct numerical simulations of the partial-differential-equation system (Eqs. 2 through 8) using a split-implicit finite-difference scheme with initial temperatures high enough for ignition to occur. The reaction-leading- and reaction-trailing-wave structures were observed for different oil concentrations in the initial reservoir and oxygen fractions in the injected gas. Simulations showed that the reaction wave may be oscillatory for some values of parameters belonging to the region of partial-oxygen consumption in Fig. 5. When reaction waves are stable, the expected accuracy of 5–10% for the analytic solution was confirmed. Stability studies for dry combustion waves were performed by Aldushin and Kasparyan (1981) and Matkowsky and Sivashinsky (1978), which showed that a Hopf bifurcation leading to oscillatory regimes occurs for increasing Zeldovich number. Using these results, stability conditions for a steady-traveling reaction wave in our model can be obtained; see Mailybaev et al. (2010).

Conclusions

We derived analytical formulas for in-situ forward combustion by air injection in porous media containing crude oil and water. The oil components are grouped into precoke, medium-oil, and light-oil pseudocomponents. These pseudocomponents participate in different chemical and physical processes. Precoke is converted to coke at high temperatures; medium-oil components are cracked at slightly lower temperatures, releasing gaseous oil; and light-oil components and water are vaporized. Heat is released mainly in

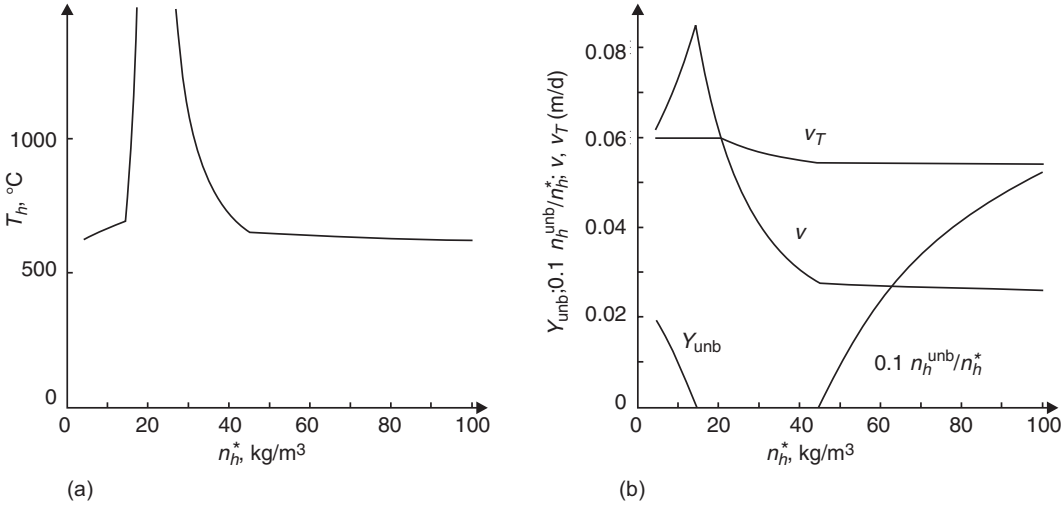

Fig. 6—HTO and thermal-wave parameters depending on precoke concentration n_h^* in kg/m³ with n_c^* = 100 kg/m³, and n_v^* = 60 kg/m³ for injection of air with reduced oxygen (2.5%). The hot-zone temperature is T_h in °C. The HTO and thermal-wave speeds are denoted by v and v_T, respectively, in m/d. The unburned-oxygen fraction is Y_{unb}. The unburned-coke fraction is n_h^{unb}/n_h^*.

the high-temperature oxidation of coke. The main assumptions used in the model are:

- Immobile oil with the composition described by three pseudo-components (i.e., heavy oil, which combusts; medium oil, which cracks; and light oil, which vaporizes).
- Only gas, which includes cracked and vaporized hydrocarbons, is moving.
- We model HTO combustion as a single reaction that depends linearly on the oxygen and fuel concentration.
- The temperature dependence can be modeled with the Arrhenius reaction equation.
- The composition in the downstream vapor zone is assumed to be given.
- The HTO reaction is the dominant heat source in the reaction wave.
- Both HTO and cracking are characterized by large Zeldovich numbers [i.e., large activation temperature (E/R) divided by the HTO zone temperature].
- Reactions at low temperatures and gas reactions are disregarded.
- Combustion occurs in a wave traveling with constant speed; all sorts of instabilities are not taken into account.
- Heat losses are disregarded.
- We ignore LTO in the case of incomplete oxygen consumption in the HTO reaction.

When heat losses are taken into account in the reaction-leading structure, the reaction wave will be relatively unaffected because it is short. However, heat loss occurs between the thermal wave upstream and the reaction wave downstream. As a result, the temperature decreases in the upstream direction from the HTO temperature to much lower values. This, however, has a minor influence on the overall behavior of the combustion zone. The effect of heat losses for a reaction-trailing structure is more complicated and outside the scope of this paper. Gas-diffusion effects are much less at typical high-pressure field conditions (the diffusion coefficient is, to an excellent approximation, inversely proportional to the pressure) and, therefore, are considered to be negligible. However, even large diffusion is shown to be of minor influence for a reaction-leading structure.

The solutions are found in the form of sequences of waves. It turns out that it is possible to distinguish between two combustion regimes according to the relative position of the hot zone and high-temperature oxidation region: reaction-leading and reaction-trailing wave structures. At low precoke concentrations or high injected-oxygen fractions, the HTO region lies downstream of the hot zone and all the coke is consumed. At high precoke concentrations or low injected-oxygen fractions, the HTO region lies upstream of the hot zone and all the oxygen is consumed. Each structure occurs in two different combustion regimes. In the first regime, both coke and oxygen are completely consumed in the combustion. In the second regime, only a part of the oxygen is consumed for the reaction-leading-wave structure, or a part of the coke is consumed for the reaction-trailing-wave structure. The typical chart with four combustion regimes is shown in Fig. 5.

We derived explicit analytical conditions for each combustion regime, as well as formulas describing dependent variables in the wave-sequence solutions. Additionally, we described the internal structure of the oil-cracking zone for the reaction-leading-wave structure. We developed a simplified method for analysis of the combustion region presented in Appendices A through C. In this method, rather than explicitly integrating wave equations, we use general estimates and exploit strong exponential dependence of combustion rate on temperature to simplify the results. This procedure is general and can be applied to the analysis of reaction zones characterized by large Zeldovich numbers, as we did in this paper for the high-temperature oxidation and cracking regions.

Numerical computations with typical reservoir data for in-situ combustion lead to the following observations. The most typical wave structure is reaction-leading. With increasing coke concentration, the partial-oxygen-consumption regime changes into the complete coke and oxygen consumption regime. The first regime is characterized by weak dependence of combustion temperature on reservoir parameters, while the temperatures may become very high in the complete coke and oxygen consumption regime. The reaction-trailing structure is found when the injected air contains reduced amounts of oxygen (for example, for injection of a mixture of air and flue gas). Numerical simulation of the full system of governing equations for our model was carried out showing the expected accuracy of our analytic formulas and verifying stability. For some reservoir parameters, the reaction wave turned out to be unsteady, and combustion occurred in a wave traveling with a speed changing periodically in time.

The main limitation of the current paper is that it does not incorporate LTO in the case of incomplete oxygen consumption. However, Fig. 5 helps to understand the conditions for which incomplete oxygen consumption can be expected.

The work described has the following practical applications: validation of numerical-simulation programs, accurate risk assessment of oxygen breakthrough by anayzing the detailed structure of the reaction zone avoiding numerical artifacts, and quick evaluations of consequences of different injection conditions given the kinetic behavior of the oil under consideration.

Acknowledgments

J. Bruining is supported by the Hydrogen Oriented Underground Coal Gasification for Europe (HUGE) project, which, in turn, is supported by the EU Research Fund for Coal and Steel under Contract RFCR-CT-2007-00006 and the Polish Ministry of Science and Higher Education. This work is also supported in part by Brazil's National Council for Scientific and Technological Development under Grants 301564/2009-4, 472923/2010-2, 490707/2008-4, 474121/2008-9, 314583/2009-2, and 301564/2009-4; Fundação de Amparo À Pesquisa do Estado do Rio de Janeiro under Grants E-26/110.972/2008, E-26/102.723/2008, E-26/112.220/2008, E-26/110.310/2007, and E-26/112.112/2008; and the President of Russian Federation Grant. The authors also thank the Instituto Nacional de Matemática Pura e Aplicada in Rio de Janeiro and Delft University of Technology for hospitality during the visits.

References

Abou-Kassem, J.H., Farouq Ali, S.M., and Ferrer, J. 1986. Appraisal of Steamflood Models. *Rev. Téc. Ing. Univ. Zulia* **9**: 45–58.

Abu-Khamsin, S.A., Brigham, W.E., and Ramey, H.J. Jr. 1988. Reaction Kinetics of Fuel Formation for In-Situ Combustion. *SPE Res Eng* **3** (4): 1308–1315. SPE-15736-PA. doi: 10.2118/15736-PA.

Adagulu, G.D. and Akkutlu, I.Y. 2007. Influence of In-Situ Fuel Deposition on Air Injection and Combustion Processes. *J Can Pet Technol* **46** (4): 54–61. JCPT Paper No. 07-04-06. doi: 10.2118/07-04-06.

Akin, S., Kok, M.V., Bagci, S., and Karacan, Ö. 2000. Oxidation of Heavy Oil and Their SARA Fractions: Its Role in Modeling In-Situ Combustion. Paper SPE 63230 presented at the SPE Annual Technical Conference and Exhibition, Dallas, 1–4 October. doi: 10.2118/63230-MS.

Akkutlu, I.Y. and Yortsos, Y.C. 2000. The Dynamics of Combustion Fronts in Porous Media. Paper SPE 63225 presented at the SPE Annual Technical Conference and Exhibition, Dallas, 1–4 October. doi: 10.2118/63225-MS.

Akkutlu, I.Y. and Yortsos, Y.C. 2003. The Dynamics of In-Situ Combustion Fronts in Porous Media. *Combustion and Flame* **134** (3): 229–247. doi: 10.1016/S0010-2180(03)00095-6.

Akkutlu, I.Y. and Yortsos, Y.C. 2004. Steady-State Propagation of In-Situ Combustion Fronts with Sequential Reactions. Paper SPE 91957 presented at the SPE International Petroleum Conference in Mexico, Puebla, Mexico, 7–9 November. doi: 10.2118/91957-MS.

Akkutlu, I.Y. and Yortsos, Y.C. 2005. The Effect of Heterogeneity on In-Situ Combustion: Propagation of Combustion Fronts in Layered Porous Media. *SPE J.* **10** (4): 394–404. SPE-75128-PA. doi: 10.2118/75128-PA .

Aldushin, A.P. and Kasparyan, S.G. 1981. Stability of Stationary Filtrational Combustion Waves. *Combustion, Explosion, and Shock Waves* **17** (6): 615–625. doi: 10.1007/BF00784250.

Aldushin, A.P., Bayliss, A., and Matkowsky, B.J. 2006. On the Transition from Smoldering to Flaming. *Combustion and Flame* **145** (3): 579–606. doi: 10.1016/j.combustflame.2005.12.009.

Aldushin, A.P., Matkowsky, B.J., and Schult, D.A. 1996. Downward Buoyant Filtration Combustion. *Combustion and Flame* **107** (1–2):151–175. doi: 10.1016/0010-2180(96)00093-4.

Aldushin, A.P., Matkowsky, B.J., and Schult, D.A. 1997. Buoyancy Driven Filtration *Combustion. Combustion Science and Technology* **125** (1): 283–349. doi: 10.1080/00102209708935662.

Bagci, S. and Kok, M.V. 2004. Combustion Reaction Kinetics of Turkish Crude Oils. *Energy & Fuels* **18** (5): 1472–1481. doi: 10.1021/ef040014g.

Bayliss, A. and Matkowsky, B.J. 1994. From Traveling Waves to Chaos in Combustion. *SIAM J. Appl. Math.* **54** (1): 147–174. doi: 10.1137/S0036139992232921.

Bousaid, I.S. and Ramey, H.J. Jr. 1968. Oxidation of Crude Oil in Porous Media. *SPE J*. **8** (2): 137–148; *Trans.*, AIME, **243.** SPE-1937-PA. doi: 10.2118/1937-PA.

Bowes, P.C. and Thomas, P.H. 1966. Ignition and Extinction Phenomena Accompanying Oxygendependent Self-Heating of Porous Bodies. *Combustion and Flame* **10** (3): 221–230. doi: 10.1016/0010-2180(66)90078-2.

Bruining, J., Mailybaev, A.A. and Marchesin, D. 2009. Filtration Combustion in a Wet Porous Medium. *SIAM J. Appl. Math*. **70** (4): 1157–1177. doi: 10.1137/080741318.

Byrne, H. and Norbury, J. 1997. The Effect of Solid Conversion on Travelling Combustion Waves in Porous Media. *Journal of Engineering Mathematics* **32** (4): 321–342. doi: 10.1023/A:1004261121570.

Castanier, L.M. and Brigham, W.E. 1997. Modifying In-Situ Combustion with Metallic Additives. *In Situ* **21**: 27–45.

Castanier, L.M. and Brigham, W.E. 2003. Upgrading of Crude Oil Via In Situ Combustion. *Journal of Petroleum Science and Engineering* **39** (1–2): 125–136. doi: 10.1016/S0920-4105(03)00044-5.

Dietz, D.N. and Bruining, J. 1981. In Situ Gasification with Heat Recuperation by Cold Water Injection. Paper SPE 10187 presented at the SPE Annual Technical Conference and Exhibition, San Antonio, Texas, USA, 4–7 October. doi: 10.2118/10187-MS.

Dietz, D.N. and Weijdema, J. 1968. Wet and Partially Quenched Combustion. *J Pet Technol* **20** (4): 411–415. SPE-1899-PA. doi: 10.2118/1899-PA.

Gerritsen, M.A. and Durlofsky L.J. 2005. Modeling Fluid Flow in Oil Reservoirs. *Annual Review of Fluid Mechanics* **37**: 211–238. doi: 10.1146/annurev.fluid.37.061903.175748.

Gutiérrez, D., Moore, R.G., Mehta, S.A., Ursenbach, M.G., and Skoreyko, F. 2009. The Challenge of Predicting Field Performance of Air Injection Projects Based on Laboratory and Numerical Modelling. *J Can Pet Technol* **48** (4): 23–33. PETSOC-09-04-23-DA. doi: 10.2118/09-04-23-DA.

He, B., Chen, Q., Castanier, L.M., and Kovscek, A.R. 2005. Improved In-Situ Combustion Performance With Metallic Salt Additives. Paper SPE 93901 presented at the SPE Western Regional Meeting, Irvine, California, USA, 30 March–1 April. doi: 10.2118/93901-MS.

Kok, M.V. and Karacan, C.O. 2000. Behavior and Effect of SARA Fractions of Oil during Combustion. *SPE Res Eval & Eng* **3** (5): 380–385. SPE-66021-PA. doi: 10.2118/66021-PA.

Kristensen, M.R., Gerritsen, M.G., Thomsen, P.G., Michelsen, M.L., and Stenby, E.H. 2007. Efficient Integration of Stiff Kinetics With Phase Change Detection for Reactive Reservoir Processes. *Transport in Porous Media* **69** (3): 383–409. doi: 10.1007/s11242-006-9079-y.

Kuhn, C.S. and Koch, R.L. 1953. In-Situ Combustion: Newest Method of Increasing Oil Recovery. *Oil & Gas Journal* **52** (14): 92.

Lin, C.Y., Chen, W.H., and Culham, W.E. 1987. New Kinetic Models for Thermal Cracking of Crude Oils in In-Situ Combustion Processes. *SPE Res Eng* **2** (1): 54–66. SPE-13074-PA. doi: 10.2118/13074-PA.

Lin, C.Y., Chen, W.H., Lee, S.T., and Culham, W.E. 1984. Numerical Simulation of Combustion Tube Experiments and the Associated Kinetics of In-Situ Combustion Processes. *SPE J.* **24** (6): 657–666. SPE-11074-PA. doi: 10.2118/11074-PA.

Mailybaev, A.A., Bruining, J., and Marchesin, D. 2010. Analysis of In Situ Combustion of Oil with Pyrolysis and Vaporization. *Combustion and Flame.* doi: 10.1016/j.combustflame.2010.10.025.

Mamora, D.D. 1995. New Findings in Low-Temperature Oxidation of Crude Oil. Paper SPE 29324 presented at the SPE Asia Pacific Oil and Gas Conference, Kuala Lumpur, 20–22 March. doi: 10.2118/29324-MS.

Mamora, D.D. and Brigham, W.E. 1995. Effect of Low-Temperature Oxidation on the Fuel and Produced Oil during In-Situ Combustion of a Heavy Oil. *In Situ* 19 (4): 341–365.

Matkowsky, B.J. and Sivashinsky, I.G. 1978. Propagation of a Pulsating Reaction Front in Solid Fuel Combustion. *SIAM J. Appl. Math*. **35** (3): 465–478. doi: 10.1137/0135038.

Pant, K.K. and Kunzru, D. 1996. Pyrolysis of n-heptane: Kinetics and Modeling. *Journal of Analytical and Applied Pyrolysis* **36** (2): 103–120. doi: 10.1016/0165-2370(95)00925-6.

Ramey, H.J. Jr. 1954. Discussion (Development of an Underground Heat Wave for Oil Recovery). *J Pet Technol* (May): 32–33.

Schult, D.A., Bayliss, A., and Matkowsky, B.J. 1998. Traveling waves in natural counterflow filtration combustion and their stability. *SIAM J. Appl. Math*. **58** (3): 806–852.

Schult, D.A., Matkowsky, B.J., Volpert, V.A., and Fernandez-Pello, A.C. 1996. Forced Forward Smolder Combustion. *Combustion and Flame* **104** (1–2): 1–26. doi: 10.1016/0010-2180(95)00102-6.

Smith, I.W. 1978. The Intrinsic Reactivity of Carbons to Oxygen. *Fuel* **57** (7): 409-414. doi: 10.1016/0016-2361(78)90055-8.

Wahle, C.W., Matkowsky, B.J., and Aldushin, A.P. 2003. Effects of Gas-Solid Nonequilibrium in Filtration Combustion. *Combustion Science and Technology* **175** (8): 1389–1499. doi: 10.1080/00102200390218921.

Weijdema, J. 1968. Zur oxydationskinetik kohlenwasserstoffe in porTosen medien in bezug auf untererdische verbrennung. *Erdol und Kohle, Erdgas Petrochemie* **21**: 520–526.

Zeldovich, Y.B., Barenblatt, G.I., Librovich, V.B., and Makhviladze, G.M. 1985. *The Mathematical Theory of Combustion and Explosion*. New York: Consultants Bureau.

Appendix A—HTO Region

The region where HTO takes place in a combustion wave contains coke and injected gas with oxygen, combustion products, and some inert gas. The highest temperature in the reservoir T_h is reached in this region. Because all medium- and light-oil components are cracked and vaporized downstream, the molar gas flux in the HTO region is the injected-gas flux $(\rho u)_{\text{inj}}$. It remains constant because one mole of O_2 is converted to one mole of CO_2. The injected-oxygen molar flux is $(\rho u Y)_{\text{inj}}$. The coke concentration ahead of the HTO region is n_h^*.

The reaction rate (Eq. 7) has strong temperature dependence determined by the exponent. Therefore, we can afford only a very small temperature variation δT_h in the reaction zone. Expanding the exponent near T_h, for small $\delta T_h = T_h - T$, we find

$$\exp\left(-\frac{E_h}{RT}\right) \approx \exp\left(-\frac{E_h}{RT_h}\right)\exp\left[-\frac{Z_h \delta T_h}{(T_h - T_v)}\right], \quad \ldots\ldots\ldots\ldots (A\text{-}1)$$

with

$$Z_h = E_h (T_h - T_v)/(RT_h^2), \quad \ldots\ldots\ldots\ldots\ldots\ldots\ldots\ldots (A\text{-}2)$$

where $Z_h >> 1$ because the activation energy E_h is large (a typical value is $Z_h \sim 15$). The last exponential in Eq. A-1 is a reduction factor in the reaction rate, and the reaction ceases when this factor becomes small. Thus, the reaction occurs within a small temperature interval $\delta T_h \sim (T_h - T)/Z_h$ that corresponds to a change of order 1 in the exponent; the reaction rate decreases rapidly and becomes negligibly small for lower $T < T_h - \delta T_h$. The dimensionless quantity Z_h is the Zeldovich number, the ratio of the total temperature variation in the wave to the temperature variation in the HTO region (Zeldovich et al. 1985). Using the expression for δT_h, we find that the HTO reaction is confined within the space interval given by

$$\delta x_h \sim \delta T_h / |T_h'| \sim (T_h - T_v)/(Z_h |T_h'|), \quad \ldots\ldots\ldots\ldots\ldots (A\text{-}3)$$

where $|T_h'|$ is the effective temperature gradient in the HTO region (the prime denotes the derivative $\partial/\partial x$). For $Z_h >> 1$, δx_h is much smaller than the width of the whole wave, which is estimated as $(T_h - T_v)/|T_h'| \sim Z_h \delta x_h$, so the HTO region is thin.

The maximal concentrations of coke and oxygen in the HTO region equal n_h^* and Y_{inj}, and at least one of them is completely consumed in the reaction. Thus, using the estimate $Yn_f \sim Y_{inj}n_f^*/2$ and $T \approx T_h$ in Eq. 7, we find the effective HTO rate in the combustion zone:

$$W_h^* \sim K_h\left(Y_{inj}n_h^*/2\right)\exp\left[-E_h/\left(RT_h\right)\right]. \quad \text{.....(A-4)}$$

Note that the exponent in this expression is very sensitive to T_h. It changes by order when T_h is changed by $2(T_h-T_v)\,Z_h^{-1}$. Hence, because we are interested in obtaining the results with relative accuracy of order Z_h^{-1} for T_h, the ~ sign in such an expression can be replaced by an equality. This fact is the key idea that allows making approximations that appear to be correct only in order of magnitude but which actually give rise to Z_h^{-1} errors only. It will be used repeatedly further on.

Complete Consumption of Coke and Oxygen. In the case of complete consumption of coke and oxygen, $\upsilon n_h^*/M_h$ moles of coke burn per unit time and per unit wave-surface area, where υ is the combustion-wave speed. For the reaction $C+O_2 \rightarrow CO_2$, it is equal to the molar oxygen flux $(\rho u Y)_{inj}$ in the injected air. This determines the combustion-propagation speed in Eq. 11.

The temperature gradient vanishes on one side of the HTO region. On the other side, it can be estimated by balancing the heat $Q_h n_h^* \upsilon$ generated per unit time with the heat flux $\lambda T'$ because of heat conductivity. This comparison yields $T' = -Q_h n_h^* \upsilon/\lambda$. The heat transferred by the flowing gas is not important here because the changes of gas flux and temperature in the thin HTO region are small; see Figs. 2 and 3. The average gradient in the HTO region, therefore, is

$$\left|T_h'\right| \sim Q_h n_h^* \upsilon/(2\lambda) = Q_h\left(\rho u Y\right)_{inj} M_h/(2\lambda). \quad \text{.....(A-5)}$$

Using Eqs. A-2 and A-5 in Eq. A-3, we find the width of the reaction zone:

$$\delta x_h \sim \frac{2\lambda RT_h^2}{E_h Q_h\left(\rho u Y\right)_{inj} M_h}, \quad \text{.....(A-6)}$$

which is determined by the temperature dependence of the reaction rate.

We sketch the derivation for Eq. 12 as follows. Because the amount of oxygen equals the amount of carbon consumed, we can use Eqs. 7 and 4 with the time derivative term neglected to show that

$$-\frac{\partial \ln Y}{\partial x} = \frac{W_h}{\rho u Y M_h} \sim \frac{K_h n_h^*}{2\left(\rho u\right)_{inj} M_h}\exp\left(-\frac{E_h}{RT_h}\right). \quad \text{.....(A-7)}$$

Integration over the interval δx_h, essential for the HTO reaction, leads to

$$\ln\left(\frac{Y_{inj}}{Y_{unb}}\right) \sim \frac{K_h n_h^*}{2\left(\rho u\right)_{inj} M_h}\exp\left(-\frac{E_h}{RT_h}\right)\delta x_h. \quad \text{.....(A-8)}$$

When the right side of Eq. A-8 exceeds unity, almost complete oxygen consumption occurs. Substitution of Eq. A-6 leads to the complete-oxygen-consumption condition (Eq. 12), where the ~ sign can be replaced by an equality with relative accuracy of order Z_h^{-1} for T_h.

Partial Oxygen Consumption. Oxygen may not be consumed in the reaction zone completely, so a considerable mole fraction Y_{unb} of oxygen remains in the gas downstream of the HTO region. The reaction-trailing structure is not possible. We have the reaction-leading case, and the flux of consumed oxygen $(Y_{inj}-Y_{unb})(\rho u)_{inj}$ reacts with an equal molar amount of coke $\upsilon n_h^*/M_h$. This yields Eq. 16.

The average temperature gradient in the HTO region is

$$|T_h'| \sim Q_h n_h^* \upsilon/(2\lambda), \quad \text{.....(A-9)}$$

as is found in Eq. A-5, except that υ is unknown. Then, Eqs. A-2 and A-3 give

$$\delta x_h \sim 2\lambda RT_h^2/\left(E_h Q_h n_h^* \upsilon\right). \quad \text{.....(A-10)}$$

In this case, both coke and oxygen are present downstream of the HTO region, where the reaction stops because of low temperature. Thus, the reaction occurs within the whole interval δx_h, and the total reaction rate is estimated as $W_h^* \delta x_h$. Equating this rate to the amount of coke $n_h^* \upsilon$ burned per unit time, we obtain Eq. 14. Here we used Eqs. A-4 and A-10 and replaced the ~ sign by an equality with relative accuracy of order Z_h^{-1} for T_h, as we did for Eq. 12.

Partial Coke Consumption. Consider the case when oxygen is consumed completely but part of the coke with concentration n_h^{unb} remains in the burned region downstream of the combustion wave. The reaction-leading structure is not possible. We have the reaction-trailing case, and the combustion-wave speed is determined by equating the burned-coke rate $\left(n_h^* - n_h^{unb}\right)\upsilon/M_h$ with oxygen flux $(\rho u Y)_{inj}$, obtaining

$$\upsilon = \left(\rho u Y\right)_{inj} M_h/\left(n_h^* - n_h^{unb}\right). \quad \text{.....(A-11)}$$

Following the same derivations as in the case of partial oxygen consumption, but with the burned-coke concentration taken as $n_h^* - n_h^{unb} = \left(\rho u Y\right)_{inj} M_h/\upsilon$, we obtain Eq. 22 instead of Eq. 14.

Appendix B—Reaction-Leading Structure

Consider the reaction-leading structure of the reaction wave. The total heat released in the reaction wave per unit time equals υQ, where

$$Q = Q_h n_h^* - Q_c n_c^* - Q_v n_v^*. \quad \text{.....(B-1)}$$

The heat rate $c_g(\rho u)_{inj}(T_h-T_{st})-c_g(\rho u)_v(T_h-T_{st})$ transported by the gas, together with Eq. B-1, contributes to the heat accumulated in the hot zone behind the reaction wave,

$$\upsilon Q + c_g\left(\rho u\right)_{inj}\left(T_h - T_{st}\right) - c_g\left(\rho u\right)_v\left(T_v - T_{st}\right) = \upsilon C_m\left(T_h - T_v\right). \quad \text{.....(B-2)}$$

Using Eqs. 9 and 10, Eq. B-2 is solved for T_h as

$$T_h = T_v + \frac{\upsilon Q}{C_m\left(\upsilon - \upsilon_T\right)}, \quad \text{.....(B-3)}$$

where we neglected the small term $-\left(T_v - T_{st}\right)c_g\upsilon\left[\left(n_c^*/M_c\right) + \left(n_v^*/M_v\right)\right]$ in the denominator. When solved for υ, Eq. B-3 leads to

$$\upsilon = \frac{\upsilon_T}{1 - Q/\left[C_m\left(T_h - T_v\right)\right]}. \quad \text{.....(B-4)}$$

For $Y_{unb} > 0$, Eq. 16 gives $\upsilon < \left(\rho u Y\right)_{inj} M_h/n_h^*$. Substituting $\upsilon = \left(\rho u Y\right)_{inj} M_h/n_h^*$ into Eq. B-3 yields a lower bound for T_h. The terms containing n_c^* and n_v^* in Q are usually small and can be neglected. This simplification is used in Eqs. 11, 13, and 15.

Cracking Region. Because of its high activation energy, the cracking reaction occurs in a thin region near the corresponding

temperature T_c. The cracking region is thin because of the cracking rate given in Eq. 8 for the data in Table 1. The analysis of the cracking region will be presented in short form because it has much in common with the analysis of the HTO region.

The reaction is mostly confined within a small temperature interval $\delta T_c \sim (T_c - T_v)/Z_c$ with a large Zeldovich number $Z_c = E_c(T_c - T_v)/(RT_c^2) >> 1$. As in Eq. A-3, the width of the cracking region is $\delta x_c = (T_c - T_v)/(Z_c|T_c'|)$, where $|T_c'|$ is the effective temperature gradient in the region. The expression for the effective cracking rate in the region is similar to Eq. A-4; i.e., $W_c^* \sim K_c(n_c^*/2)\exp[-E_c/(RT_c)]$. The cracking temperature can be found from the medium-oil balance relation $W_c^* \delta x_c \sim \upsilon n_c^*$ as Eq. 18, where the ~ sign is replaced by equality, which is a good approximation for large Z_c; see Appendix A.

The heat and gas production in the cracking zone is always small. Then, in the region between the HTO and cracking regions, $(\rho u) \approx (\rho u)_{\text{inj}}$. The heat equation (Eq. 6) takes the form

$$-\upsilon C_m T' + c_g(\rho u)_{\text{inj}} T' = \lambda T'', \quad \ldots\ldots\ldots\ldots\ldots\ldots \text{(B-5)}$$

where $\partial/\partial t = -\upsilon \partial/\partial x$ in a traveling wave moving with speed υ. Setting $x = 0$ at the HTO region, we have $T(0) = T_h$. As we showed in Appendix A in the Complete Consumption of Coke and Oxygen subsection, the temperature gradient ahead of the HTO region is $T'(0) = -Q_h n_h^* \upsilon/\lambda$. Solving Eq. B-5 with these initial conditions yields

$$T(x) = T_h + \frac{Q_h n_h^* \upsilon}{C_m(\upsilon_T - \upsilon)}\left\{1 - \exp\left[\frac{C_m(\upsilon_T - \upsilon)x}{\lambda}\right]\right\}. \quad \ldots\ldots \text{(B-6)}$$

In particular, in the cracking region, $T = T_c$ and we find Eq. 19.

In a more-detailed model of cracking, a distribution of various medium-oil components must be considered. In this case, the cracking region is wider. It is formed by thin cracking regions corresponding to all medium-oil components; see Fig. 2 (thin dark interval is a cracking region for a specific component). Note that Eqs. 18, 19, B-5, and B-6 do not contain the medium-oil concentration n_c^*. This means that they can be used to compute the temperature and position of a cracking region for each medium-oil component characterized by specific kinetic coefficients K_c and E_c.

Appendix C—Reaction-Trailing Structure

Consider now the reaction-trailing structure. The reaction wave is assumed to be a traveling wave. The only reaction in this wave is oxidation. The gas flow is uniform in the reaction wave, $\rho u = (\rho u)_{\text{inj}}$. The heat balance in the wave is described by an equation similar to Eq. B-2:

$$\upsilon Q_h(n_h^* - n_h^{\text{unb}}) + c_g(\rho u)_{\text{inj}}(T_i - T_h) = \upsilon C_m(T_i - T_h). \quad \ldots\ldots \text{(C-1)}$$

Using Eq. A-11 and solving Eq. C-1 for υ, we obtain Eq. 21.

When the coke is not consumed completely in the HTO reaction, Eq. A-11 yields the unburned-coke concentration as Eq. 24. The condition $n_h^{\text{unb}} > 0$ gives $\upsilon > (\rho u Y)_{\text{inj}} M_h / n_h^*$. Substituting this inequality into Eq. C-1 yields the lower bound given by Eq. 23.

Thermal Wave. Cracking and vaporization are heat-absorbing processes, which decrease the thermal-wave speed compared to Eq. 9. The molar gas flux ahead of the wave is given by Eq. 25. The heat-balance equation for this wave includes the heat rate $\upsilon_T(Q_c n_c^* + Q_v n_v^*)$ absorbed in cracking and vaporization, the heat $c_g(\rho u)_{\text{inj}}(T_h - T_{st}) - c_g(\rho u)_v(T_v - T_{st})$ transported by gas, and the heat $\upsilon_T C_m(T_h - T_v)$ accumulated in the rock:

$$\upsilon_T(Q_c n_c^* + Q_v n_v^*) + \upsilon_T C_m(T_h - T_v) = c_g(\rho u)_{\text{inj}}(T_h - T_{st}) - c_g(\rho u)_v(T_v - T_{st}). \quad \ldots\ldots\ldots\ldots \text{(C-2)}$$

Using Eq. 25, we solve Eq. C-2 as

$$\upsilon_T = c_g(\rho u)_{\text{inj}}/(C_m + C^*),$$

$$C^* = (Q_c n_c^* + Q_v n_v^*)/(T_h - T_v), \quad \ldots\ldots\ldots\ldots\ldots\ldots \text{(C-3)}$$

neglecting the small term $c_g(T_v - T_{st})[(n_c^*/M_c) + (n_v^*/M_v)]$ in the numerator of the second expression. In our model, the influence of cracking and vaporization given by the term C^* is usually small, so υ_T is close to the value in Eq. 9.

Appendix D—Effect of Gas Diffusion

The gas diffusion (neglected in our model) may lead to considerable change of the oxygen fraction Y within the HTO region. For the reaction-leading structure, Y is bounded by the values of the unburned- and injected-oxygen fractions, $Y_{\text{unb}} \le Y \le Y_{\text{inj}}$, and the gas diffusion may lead to variations of Y within this interval. When $Y_{\text{unb}} << Y_{\text{inj}}$ (the complete-oxygen-consumption case), the wave parameters are determined directly by the material balance of reactants, so the diffusion has no effect. In the case $Y_{\text{unb}} \sim Y_{\text{inj}}$, the value of Y remains the same by order of magnitude for arbitrary diffusion. As it follows from the analysis of the partial-oxygen-consumption case, such a change of Y leads only to small corrections of relative order Z_h^{-1} for reaction-wave parameters. Thus, within the accuracy of the method, gas diffusion (large or small) plays essentially no role in the determination of reaction-wave parameters in the case of the reaction-leading structure.

In case of the reaction-trailing structure, strong diffusion leads to the displacement of oxygen away from the reaction zone, which may affect the results. The characteristic diffusion length is $L_D = D\phi/u_{\text{inj}}$, where D in m²/s is the diffusion coefficient and u_{inj}/ϕ in m/s is the gas speed. Gas diffusion can be neglected in the analysis of the reaction-trailing structure when L_D is of the same order as or is less than the reaction-zone length given by Eq. A-10, where one can use the upper bound for υ given by Eq. 9. For reservoir parameters in Table 1 and $D = 2\times10^{-5}$ m²/s, we have $L_D/\delta x_h \sim 0.005$ m/0.1 m <<1, so the gas diffusion can be neglected.

Notice that earlier studies assumed very large (dominant) gas diffusion in the reaction-leading case [e.g., Akkutlu and Yortsos (2000, 2003) and Schult et al. (1996)] or very small (neglected) diffusion for both reaction-leading and reaction-trailing cases [e.g., Wahle et al. (2003)]. The formulas of these authors lead to the same result as ours up to the accuracy of approximation $\sim Z_h^{-1}$.

Alexei A. Mailybaev is a chief researcher at the Laboratory of Mechanics of Natural Processes in the Institute of Mechanics of the Lomonosov Moscow State University. He holds PhD and DSc degrees from the same institution. His research area is applied mathematics, including stability theory, dynamical systems, and conservation laws with applications in reactive flow in porous media and other problems of physics and mechanical engineering. **Hans Bruining** is Professor of Geo-Environmental Engineering at the Delft University of Technology. He holds MS and PhD degrees in physical chemistry from the University of Amsterdam. Bruining's current research concerns upscaled models of fractured reservoirs, modeling and experiments of thermal recovery, and experiments of thermal recovery, greenhouse gas (CO_2) application and sequestration related to fossil-fuel recovery, underground coal gasification, and application of EOR techniques for remediation of polluted soils. **Dan Marchesin** holds an MS degree from the Pontifical Catholic University of Rio de Janeiro and a PhD degree from New York University in mathematics. He is currently a researcher at the National Institute for Pure and Applied Mathematics in Rio de Janeiro, Brazil. He is interested in the mathematics and numerics of multiphase flow in porous media, including generalizations of the Buckley-Leverett theory to immiscible three-phase flow, and compositional and reactive flows. Applications include EOR and CO_2 storage.